

AutoDIR: Automatic All-in-One Image Restoration with Latent Diffusion

Yitong Jiang* Zhaoyang Zhang* Tianfan Xue Jinwei Gu

The Chinese University of Hong Kong

{ytjiang@link, zhaoyangzhang@link, tfxue@ie, jwgu@cse}.cuhk.edu.hk

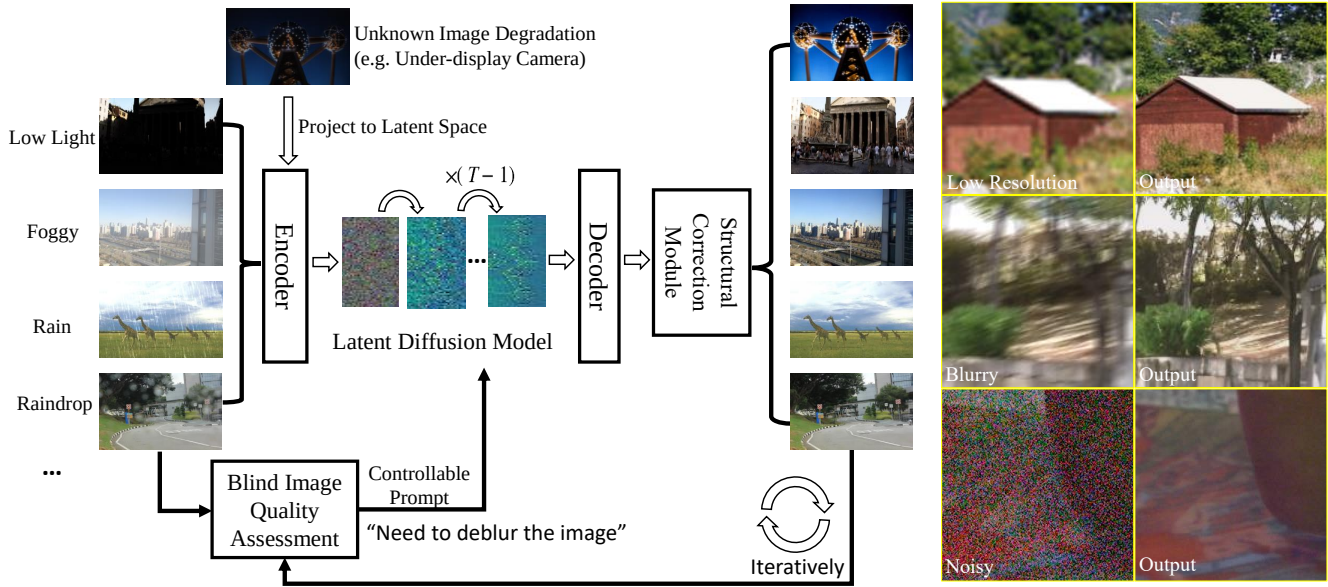


Figure 1. We propose AutoDIR, an automatic all-in-one model for image restoration that handle different degradations, including low light, foggy, etc. The left diagram shows the pipeline for multi-task image restoration via AutoDIR. First, the Blind Image Quality Assessment module (BIQA) detects the dominant artifact of the corrupted image and instructs the latent-diffusion-based All-in-One Image Editing module (AIR) with a text prompt. Then, the Structural Correction Module (SCM) enhances the edited results of the AIR for the final restored image. AutoDIR can handle images with multiple degradations through iterative repetition of the previous steps. The right column shows our model successfully restore clean images from different degradations. (**Zoom in for details**)

Abstract

In this paper, we aim to solve complex real-world image restoration situations, in which, one image may have a variety of unknown degradations. To this end, we propose an all-in-one image restoration framework with latent diffusion (AutoDIR), which can automatically detect and address multiple unknown degradations. Our framework first utilizes a Blind Image Quality Assessment Module (BIQA) to automatically detect and identify the unknown dominant image degradation type of the image. Then, an All-in-One Image Editing (AIR) Module handles multiple kinds of degradation image restoration with the guidance of BIQA. Finally, a Structure Correction Module (SCM) is

proposed to recover the image details distorted by AIR. Our comprehensive evaluation demonstrates that AutoDIR outperforms state-of-the-art approaches by achieving superior restoration results while supporting a wider range of tasks. Notably, AutoDIR is also the first method to automatically handle real-scenario images with multiple unknown degradations.

1. Introduction

Image restoration encompasses a variety of specific sub-tasks, including deblurring, denoising, deraining, super-resolution, deraindrop, and dehaze. Given the diverse nature of these subtasks, which necessitate the estimation of various image operations, prior methods [7, 19, 21, 29, 35, 41, 43, 44, 47, 54, 62, 74, 75] often train individual single-

*Equal contribution.

task models for each specific task to determine the currently estimated operation. While these single-task approaches yield promising results within their respective tasks, they encounter difficulties when applied to complex real-world situations due to: (i) Real-world images often contain multiple unknown degradations or require multiple enhancements, which cannot be addressed by a method designed for a single task. (ii) Combining multiple single-task methods can also present challenges. Users must manually identify each type of image degradation and apply the corresponding single-task model, a process that is not only inefficient but also difficult for non-professional users to navigate.

Is it possible to develop some type of “fundamental model” for image restoration with the capability for handling unknown image degradation and intuitive user control? The underlying idea is straightforward: various image restoration tasks often involve common operations, such as enhancing signal-to-noise ratio, recovering fine details, and adjusting contrast. This suggests the potential to learn a single unified model that encompasses these shared image restoration operators. Moreover, we can leverage generative models like Variational Autoencoders (VAEs) [25,58], Generative Adversarial Networks (GANs) [12], and Diffusion Models [16,48] to capture the complex empirical distributions of natural images [52]. These models have already demonstrated significant advancements in restoring image details across various image restoration tasks [11,14,38,52,62,79].

Recent literature has proposed some unified approaches to address the multi-task image restoration problem, which fall into two categories: The first category of methods [22,22,39,64] leverages pre-trained generative models, including GANs [12] and Diffusion Models [16,48], as priors. However, these methods typically require the definition or learning of an accurate explicit degradation function for each degradation type. This limitation hinders the wide applicability of these methods across diverse and complex degradation scenarios. The second category comprises end-to-end discriminative methods [26,40,71]. However, these approaches lack manual control over the type of image recovery, as they heavily rely on degradation image features for restoration guidance. Moreover, unlike generative-based image restoration methods [50,52,63], they lack the capability to hallucinate missing or deteriorated details in the images.

In this work, we propose Automatic All-in-One Image Restoration with Latent Diffusion (AutoDIR), a multi-task model that can automatically detect and deal with multiple artifacts. In addition to automatic degradation detection, we also provide a user-friendly interface that allows users to manually adjust the type of image recovery based on their specific requirements. This is achieved by utilizing recent advancements in vision-language models [20,30,45,55] and

text-to-image diffusion models [56,66,69,70], which have shown significant progress in text-to-image generation and editing but have primarily focused on semantic edits and not image quality tasks.

Specifically, our proposed pipeline comprises three stages as shown in Figure 1: (i) We fine-tune a pre-trained language-vision model CLIP [45] as a blind image quality assessment (BIQA) module to detect basic image degradation types and generate text embeddings for each image quality issue. (ii) These obtained text embeddings are then used by a text-to-image diffusion model fine-tuned to produce instruction-guided enhanced results. However, although demonstrating strong restoration and enhancement performance, we notice that the diffusion-generated outcomes exhibit noticeable instability in image textures. To tackle this problem, we incorporate (iii) a lightweight Structural-correction Module (SCM) to enhance contextual consistency.

To evaluate the effectiveness and versatility of our proposed AutoDIR, we conducted a comprehensive set of experiments encompassing seven image restoration tasks. These tasks include denoising, deblurring, low light enhancement, dehazing, deraining, deraindrop, and super-resolution. By evaluating AutoDIR’s performance on this diverse range of restoration challenges, we obtained compelling results. Our pipeline effectively identified image issues, detected artifacts, removed undesired elements, repaired damaged portions of images, and made global adjustments to the image’s appearance, all while preserving the texture details or structure.

Our contribution can be summarized as follows:

- To the best of our knowledge, this is the first work to employ a text-to-image diffusion model for addressing unified image restoration tasks.
- AutoDIR is the first model to enable automatic multi-tasking image restoration with blind image quality assessment.
- Our framework also allows for explicit user control over the image editing process through the utilization of BIQA text embeddings.
- AutoDIR is validated by comprehensive experiments across seven image restoration tasks, which is currently the highest number among unified image restoration methods.
- We conduct a thorough analysis to understand the mechanism of the language-vision model and generative diffusion model on image quality tasks.

2. Related Work

2.1. Unified Image Restoration

Previous approaches to unified image restoration can be categorized into two main groups: unsupervised genera-

tive prior-based methods [10, 22, 39, 64, 67] and end-to-end learning-based methods [9, 26, 31, 40, 59, 71].

The utilization of generative priors [3, 5, 17, 34] has been a common technique in image restoration tasks. Early methods employ generative adversarial networks (GANs) [12] for unified image restoration, which relied on GAN inversion and require manual specification of degradation models and GAN generator parameters [13, 39]. More recently, unsupervised methods [22, 64] have utilized diffusion models as priors for image restoration tasks, employing techniques such as singular value decomposition of the degradation operator or refinement of null space content during the reverse process. However, these methods are limited to linear image restoration tasks and rely on specific image degradation functions to constrain the reverse diffusion process. To address non-linear image restoration, Fei et al. [10] estimate a degradation function using gradients during the reverse process, but their applicability is limited when dealing with complex degradations like motion blur. In contrast, with a BIQA (Blind Image Quality Assessment) module, our proposed AutoDIR is able to unify complex degradations without relying on assumptions about the specific degradation functions.

The other category is end-to-end learning-based methods, which typically utilize image embeddings extracted by an auxiliary degradation predictor to guide the image restoration model [26, 31, 40, 59, 71]. For example, Valanarasu et al. [59] leverage a transformer encoder to capture hierarchical features of haze, while Li et al. [27] employ a degradation classifier trained using contrastive learning. Park et al. [40] design a degradation classifier for multiple types of degradation to select appropriate Adaptive Discriminant filters, altering network parameters based on specific degradations. However, unlike AutoDIR, these methods can only unify tasks with specific degradation types, which poses challenges when dealing with a wider range of degradation types.

2.2. Text to Image Synthesis and Editing

Early works [56, 66, 69, 70, 78] on text-to-image synthesis and editing primarily relied on generative adversarial networks (GANs) [12]. Recently, developments in diffusion models [16, 48] and language-vision models [45] have led to significant progress in image synthesis and editing [6, 37, 46, 51]. The emergence of diffusion-based methods has offered new avenues for text-to-image editing, which can be broadly categorized into data-driven [4] and no-extra-data-required approaches [15, 23, 73]. In the data-driven category, Brooks et al. [4] employs a stable diffusion model fine-tuned with a large dataset of prompt and image pairs. However, it is primarily designed for semantic image editing and struggles to deliver satisfactory results in tasks related to image quality enhancement. On the other

hand, some methods focus on image editing without extra data. For instance, recent works interpolate the text embedding [23] or score estimate [73] of the input and desired images. However, it requires individual finetuning of the diffusion model for each input image, leading to time-consuming operations. Hertz et al. [15] improves editing efficiency by directly manipulating cross-attention maps without the need of per-image finetuning. However, it requires interior maps in the reversing process and is thus not applicable to real image editing. Unlike the above methods, our AutoDIR supports real image enhancement without per-image finetuning.

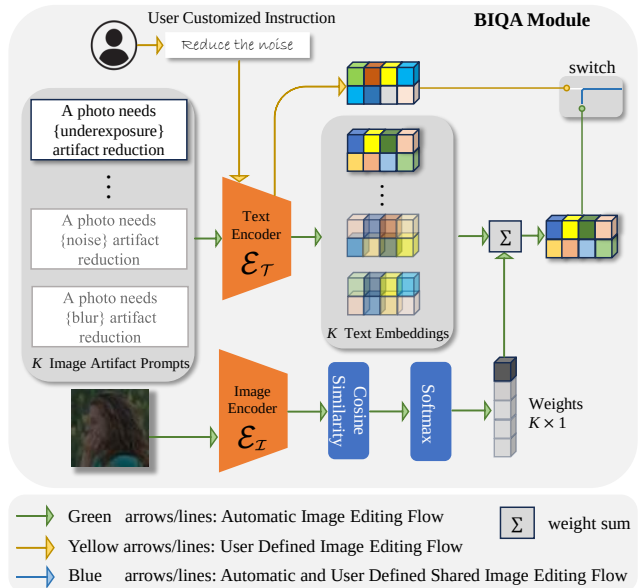


Figure 2. Illustration of the proposed Blind Image Quality Assessment Module. See Section 3 more details

3. Methodology

In this section, we introduce AutoDIR (Automatic All-in-One Image Restoration with Latent Diffusion), a versatile model that can automatically detect and address multiple unknown artifacts in images. AutoDIR consists of three key components:

(i) Blind Image Quality Assessment (BIQA) Module: The first step of AutoDIR involves the utilization of a Blind Image Quality Assessment (BIQA) module. This module automatically identifies the predominant degradation present in the input image, such as noise, blur, or compression artifacts. By analyzing the image characteristics, the BIQA module generates a corresponding text embedding, denoted as e_{auto} . This text embedding is subsequently used in the image editing process.

(ii) Image Refinement Module: After obtaining the text embedding e_{auto} , it is supplied to the image refinement

module. This module, called the diffusion-model-based all-in-one image refinement module (AIR), utilizes e_{auto} to generate an edited image, denoted as I_{sd} . The purpose of the image editing process is to specifically target and mitigate the identified degradation, thereby enhancing the overall quality of the image.

(iii) Structural-Correction Module (SCM): Finally, the edited image I_{sd} is combined with the original image I , and both are fed into the Structural-correction module (SCM). This module effectively restores the distorted context of the original image while incorporating the enhancements made during the editing phase. The output of this restoration process is the final result, denoted as I_{res} , which represents an enhanced version of the input image.

3.1. Blind Image Quality Assessment.

As illustrated in Figure 2, Let \mathcal{C} denotes the set of image distortions, i.e. $\mathcal{C} = \{c_1, c_2, \dots, c_K\}$, where c_i is an image distortion type, e.g. “noise” and K is the number of distortions we consider. The textural description prompt set is $\mathcal{T} = \{T \mid T = \text{“A photo needs } \{c_i\} \text{ artifact reduction.”}, c \in \mathcal{C}\}$. Given a corrupted image I which undergoes several unknown artifacts, our BIQA aims to identify the dominant degradation of I and extract the corresponding text embedding. We adopt a pre-trained CLIP model [45], which consists of an image encoder \mathcal{E}_I and a text encoder \mathcal{E}_T . We first obtain the image embedding $\mathcal{E}_I(I) \in \mathbb{R}^d$ and the text embedding $\mathcal{E}_T(T) \in \mathbb{R}^{K \times d}$, then we compute the cosine similarity between image embedding $\mathcal{E}_I(I)$ and each prompt embedding $\mathcal{E}_T(T_i) \in \mathbb{R}^d$ by:

$$\text{logit}(c_i|I) = \frac{\mathcal{E}_I(I) \cdot \mathcal{E}_T(T_i)}{\|\mathcal{E}_I(I)\|_2 \|\mathcal{E}_T(T_i)\|_2}, \quad (1)$$

where T_i is the i -th element of \mathcal{T} . Next, we obtain the output text embedding of BIQA e_{auto} by:

$$\hat{p}(c_i|I) = \frac{\exp(\text{logit}(c_i|I))}{\sum_{i=1}^K \exp(\text{logit}(c_i|I))} \quad (2)$$

$$e_{auto} = \sum_{i=1}^K \hat{p}(c_i|I) \mathcal{E}_T(T_i) \quad (3)$$

During the optimization of BIQA, we freeze the parameters of the text encoder \mathcal{E}_T and finetune the image encoder \mathcal{E}_I using the multi-class fidelity loss [57]. The fidelity loss can be denoted as:

$$L_{FID} = 1 - \sum_{i=1}^K \sqrt{p(c_i|I) \hat{p}(c_i|I)}. \quad (4)$$

Here, $p(c_i|I)$ is a binary variable that equals 1 if c_i is the dominant artifact in image I , and 0 otherwise.

User-customized control: Besides the automatic text embedding generated by the BIQA module (e_{auto}), we also

support user-defined prompts for customized control. Given a user instruction \mathcal{P} , we can also extract the text embedding $e_{user} = \mathcal{E}_T(\mathcal{P})$ as the guidance of the following image refinement module.

Semantic-Agnostic Constraint for Blind Image Quality Assessment.

Since the original CLIP model is pre-trained on tasks such as image classification, its corresponding $\mathcal{E}_I(I)$ encoders tend to encode images based on their semantic information (e.g., cat or dog) rather than their image quality (e.g., noisy or clean). However, when we finetune the CLIP model for generating texts for BIQA according to image quality, this differentiation becomes a significant limitation to model performance. To address this issue, we propose a novel approach called the Semantic-Agnostic constraint loss (L_{SA}) to regulate the finetuning process and prevent the model from relying solely on semantic information rather than image quality. This constraint loss can be derived using the following equation:

$$L_{SA} = \sum_{i=1}^K \sqrt{p(c_i|I) \hat{p}(c_i|I_{gt})}, \quad (5)$$

Here, I_{gt} represents the ground-truth image corresponding to the corrupted image I . $p(c_i|I)$ is a binary variable that is equal to 1 if c_i represents the dominant distortion in image I , and 0 otherwise. $\hat{p}(c_i|I_{gt})$ denotes the probability that the dominant degradation in I_{gt} is represented by c_i . The Semantic-Agnostic loss (L_{SA}) applies a penalty when the CLIP model suggests that the artifact c_i is present in the ground-truth image I_{gt} . This penalty forces the BIQA model to distinguish between I_{gt} and I based on the image quality distortion, encouraging the CLIP image encoder ($\mathcal{E}_I(I)$) to focus on extracting image quality artifact information rather than semantic information.

We incorporate the Semantic-Agnostic constraint L_{SA} with fidelity loss L_{FID} , resulting in the total loss L_{BIQA} for BIQA module:

$$L_{BIQA} = L_{FID} + L_{SA}. \quad (6)$$

The effectiveness of this constraint is further verified in Section 4.1.

3.2. All-in-one Image Editing with Latent Diffusion.

Preliminaries The Latent Diffusion Model [48] is a variant of Denoising Diffusion Probabilistic Models [16], that conducts forward and reverse processes in the latent space of a pre-trained Variational Autoencoder (VAE) [25] with an encoder \mathcal{E}_{ldm} and decoder \mathcal{D} . Given an image x , \mathcal{E}_{ldm} encodes it into a latent representation $z = \mathcal{E}_{ldm}(x)$. Then, the model follows a standard DDPM to produce a noisy latent z_t and learns to predict the added noise to z_t with denoising model $\epsilon_\theta(x_t, t)$. The optimization function of $\epsilon_\theta(x_t, t)$ is:

$$L_{ldm} = \mathbb{E}_{\mathcal{E}_{ldm}(x), \epsilon \sim \mathcal{N}(0,1), t} [\|\epsilon - \epsilon_\theta(z_t, t)\|_2^2], \quad (7)$$

where ϵ is the noise sample to be estimated, and t is the time step.

Moreover, to support conditional generation, LDM augments the UNet backbone [49] with a cross-attention mechanism [60]. The conditional latent diffusion model is learned via:

$$L_{ldm} = \mathbb{E}_{\mathcal{E}_{ldm}(x), \epsilon \sim \mathcal{N}(0,1), t} [\|\epsilon - \epsilon_{\theta}(z_t, t, y)\|_2^2], \quad (8)$$

where y is text embedding condition in our setup.

All-in-one Image Editing Our All-in-one Image Editing (AIR) module utilizes both text and image embeddings to generate diffusion priors I_{sd} via image editing. The text embedding condition, denoted as $e = \{e_{auto}, e_{user}\}$, aims to provide guidance for the editing process to disentangle different image restoration tasks, while the latent space image embedding condition $z_I = \mathcal{E}_{ldm}(I)$ from the image encoder \mathcal{E}_{ldm} of the original conditional latent diffusion model (CLDM), is to provide information of the image to be edited.

To enable the text condition to guide different image restoration editing, we incorporate cross-attention to map the text condition e into the intermediate layers of the time-conditional UNet backbone of CLDM [49]. We find that different text conditions can yield corresponding different attention maps during the reversing process, which will further alternate the sampling results and disentangle different restoration tasks. We discuss more about the mechanism of multi-task image restoration via one single diffusion-based model in Section 4.1. For the image condition, we concatenate the image condition z_I with the noisy latent z_t and feed them to the UNet backbone. Consequently, the denoiser expression of the UNet backbone becomes $\epsilon_{\theta}(e, [z_t, z_I], t)$, where $[\cdot]$ denotes concatenation.

After the reversing process, we can obtain the intermediate result I_{sd} as our diffusion priors by passing the edited latent \hat{z} through the LDM decoder \mathcal{D} , defined as $I_{sd} = \mathcal{D}(\hat{z})$.

During training, we fine-tune the UNet backbone $\epsilon_{\theta}(e, [z_t, z_I], t)$ for image restoration tasks. The objective function is defined as:

$$L_{AIR} = \mathbb{E}_{\mathcal{E}_{ldm}(x), c_I, e, \epsilon, t} [\|\epsilon - \epsilon_{\theta}(e, [z_t, z_I], t)\|_2^2]. \quad (9)$$

3.3. Structural-correction Module.

To address the contexture distortion caused by the AIR generative model, we employ an efficient Structural-correction Module (SCM) model denoted as \mathcal{F} . The purpose of SCM is to extract the contextual information \mathcal{R} from the original image and incorporate it with the intermediate image editing result I_{sd} in a residual manner. This is achieved through the following equation:

$$I_{res} = I_{sd} + w \cdot \mathcal{F}([I_{sd}, I]). \quad (10)$$

Here, $[\cdot]$ denotes concatenation, and w is an adjustable coefficient that ranges between 0 and 1. The value of w determines the extent to which contextual information is utilized to recover the final result. A larger value of w emphasizes the use of contextual information, which is beneficial for tasks that require structure-consistency, such as low light enhancement. Conversely, a smaller value of w is often employed to maintain the generation capability of AIR for tasks like super-resolution.

By integrating SCM, AutoDIR effectively restores the distorted context of the original image, seamlessly incorporating the enhancements made during the editing phase. For more results, please refer to Section 4.4.

When training SCM, instead of sampling the edited latent \hat{z}_t , which is time-consuming, we utilize the estimated edited latent \tilde{z} , which is calculated by:

$$\tilde{z} = \frac{z_t}{\sqrt{\bar{\alpha}}} - \frac{\sqrt{1 - \bar{\alpha}} \epsilon_{\theta}(e, [z_t, z_I], t)}{\sqrt{\bar{\alpha}}}. \quad (11)$$

Here, $\bar{\alpha}$ represents the noise scheduler introduced in [48]. The loss function for SCM is further defined as:

$$L_{SCM} = \|I_{gt} - (\mathcal{F}(\mathcal{D}(\tilde{z}), I) + \mathcal{D}(\tilde{z}))\|_2^2 \quad (12)$$

4. Experiments

In this section, we first conduct a meticulous analysis to gain deeper insights into the working mechanism of AutoDIR to demonstrate how AutoDIR operates. Furthermore, we perform an extensive assessment of the proposed AutoDIR framework across seven different image restoration and enhancement tasks. To fully validate the feasibility and effectiveness of unifying multiple restoration and enhancement tasks, we compare AutoDIR with both CNN-based and Diffusion-based multitasking backbones. This comparative analysis allows us to assess the performance of AutoDIR and its BIQA module. Finally, we conduct ablation studies to demonstrate the effectiveness of our pipeline.

4.1. Feasibility Analysis

Feasibility of BIQA using Vision-language Model. In our study, we begin by evaluating the effectiveness of our Vision-Language BIQA models in detecting different artifacts. Figure 4 provides a t-SNE visualization that demonstrates the separation of image feature embeddings corresponding to various artifacts and degradations. The distinct separation of embeddings from different tasks indicates the potential of regressing a BIQA model based on these image embeddings. Furthermore, Figure 5 evaluates the ability of our BIQA model to cluster embeddings based on the specific artifact itself, e.g. haze degradation in SOTs [28] dehazing dataset, rather than the content differences across different datasets. This finding further validates the effectiveness of our BIQA model.

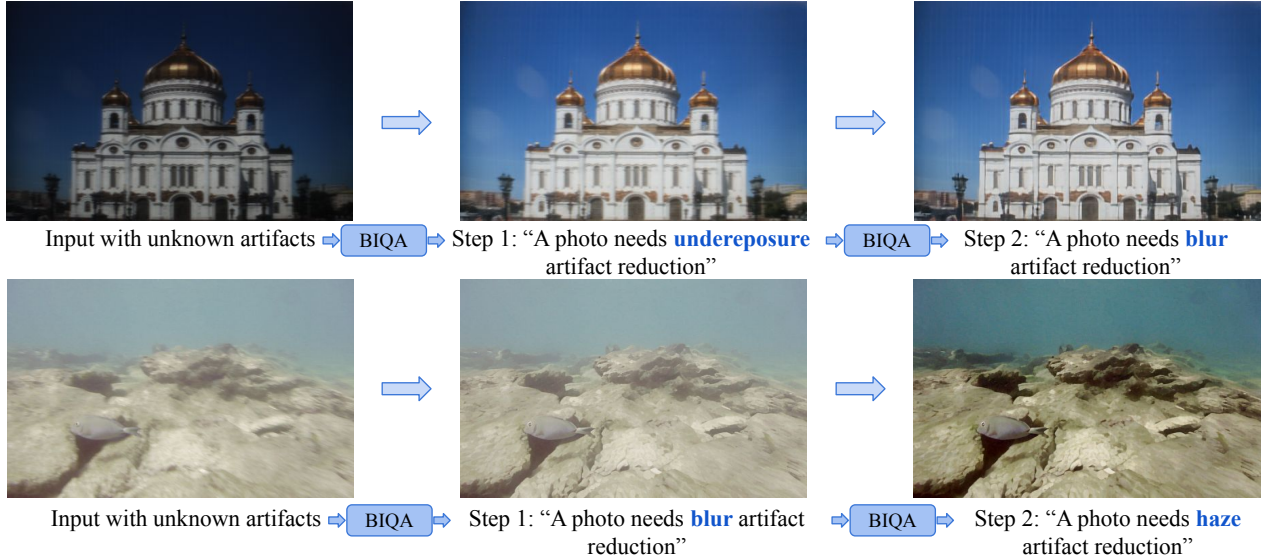


Figure 3. **Iterative image editing on unseen Under-Display Camera dataset TOLED [76] and unseen Enhancing Underwater Visual Perception (EUVP) dataset [18].** Left column: input image with unknown artifacts. Medium column: step-one edited images after brightening/deblurring based on the input image. Right column: step-two edited images after deblurring/dehazing based on one step-one edited image

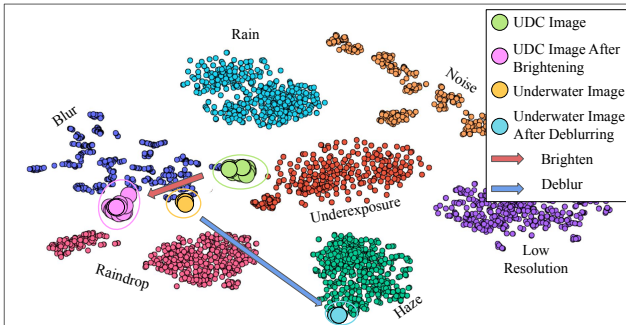


Figure 4. **t-SNE visualization of image embeddings on images with seven degradation types, unseen Under-Display Camera (UDC) dataset TOLED [76] and unseen Enhancing Underwater Visual Perception (EUVP) dataset [18].** Embeddings of UDC input images, which contain blur and underexposure artifacts, are distributed between blur and underexposure areas. After step-one editing, they shift to the blurred artifact area, which indicates that the underexposure artifact is removed. Embeddings of EUVP input images are distributed in the blurred artifact area and move to the haze area after the deblurring operation, which indicates that the blur artifact is removed and the haze artifact is the remaining dominant degradation.

Such behavior has been observed to be associated with finetuning with the Semantic-agnostic constraint. Specifically, before and after finetuning without Semantic-agnostic constraint, the feature extracted from degraded images cannot be distinguished from clean images, indicating a focus on the semantic information. However, after our finetuning without SA constraint, the degraded image embeddings can

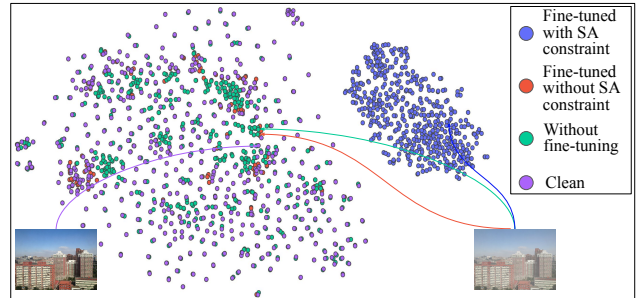


Figure 5. **t-SNE visualization of image embedding of image assessment module on SOT's dehazing dataset [28].** Degraded image embedding of BIQA image encoder fine-tuned with Semantic-agnostic constraint can be separated from clean image embedding, while image embedding of image assessment module fine-tuned without SA constraint or without fine-tuning mixes up with image embedding of clean images. This indicates the effectiveness of our SA constraint to regularize the BIQA image encoder to extract information on quality artifacts instead of semantic content.

be separated from the clean image embeddings, showing improved artifact detection.

Handling multiple unknown artifacts. The AutoDIR pipeline is able to handle **multiple unknown** artifacts. To demonstrate this, we conduct experiments on an unseen under-display-camera dataset [77] and unseen Enhancing Underwater Visual Perception (EUVP) dataset [18] containing various unknown artifacts. In Figure 3, we demonstrate the iterative process of our image assessment model. For the UDC image, it first suggests the brightening underexposed image and then proceeds to detect and deblur blurry

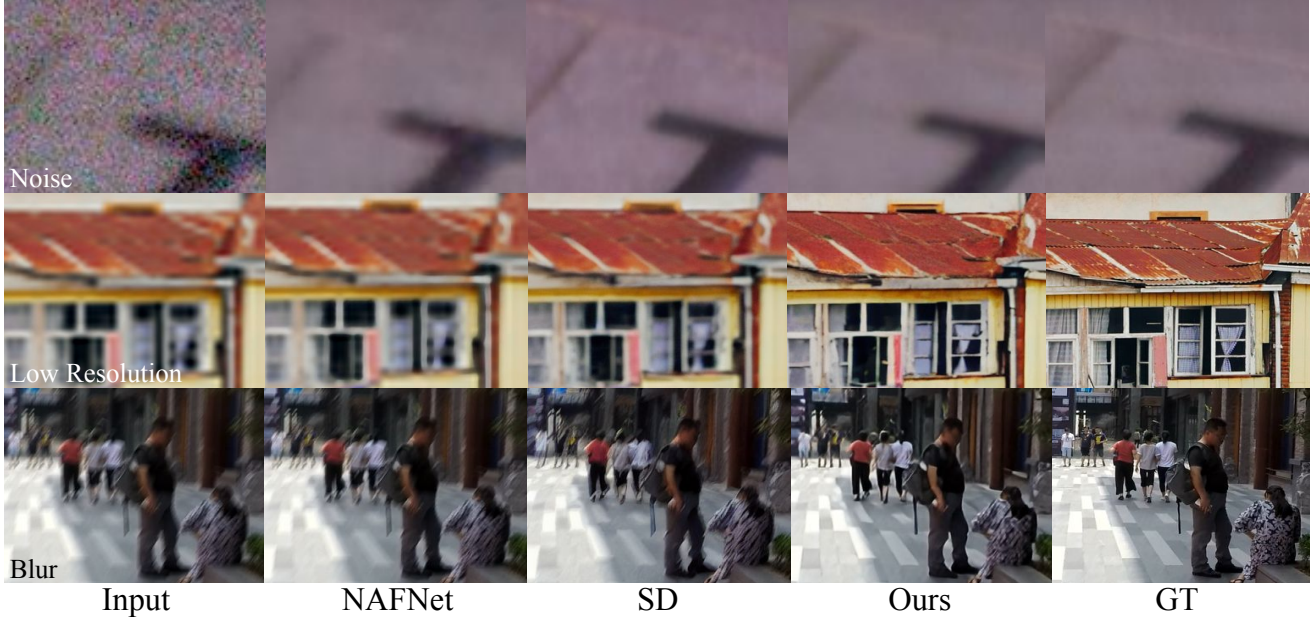


Figure 6. Qualitative comparisons with NAFNet [8] and Stable Diffusion (SD) [48] on denoising, $\times 8$ super-resolution, and deblurring tasks. See the Appendix for more results (**Zoom in for better view**).

Table 1. Quantitative comparison on denoising, deraining, dehaze, deraindrop and low light enhancement tasks. PSNR/SSIM \uparrow : the higher, the better; LPIP \downarrow : the lower, the better. The best and second-best performances are marked in red and blue.

Method	Denoise						Derain			Dehaze			Deraindrop			Low light		
	Real			Synthetic $\sigma = 25$			PSNR	SSIM	LPIPS	PSNR	SSIM	LPIPS	PSNR	SSIM	LPIPS	PSNR	SSIM	LPIPS
	PSNR	SSIM	LPIPS	PSNR	SSIM	LPIPS												
AirNet (3 Tasks)	16.47	0.301	0.855	30.99	0.898	0.103	34.31	0.952	0.039	27.67	0.965	0.029	-	-	-	-	-	-
NAFNet	37.08	0.921	0.165	29.35	0.864	0.138	30.46	0.926	0.100	26.75	0.948	0.038	25.04	0.872	0.138	21.15	0.837	0.240
Stable Diffusion	32.64	0.874	0.126	23.23	0.627	0.150	23.21	0.651	0.147	23.49	0.763	0.091	24.84	0.738	0.104	18.97	0.770	0.159
Ours	36.91	0.919	0.145	30.12	0.885	0.093	33.05	0.954	0.036	28.14	0.962	0.021	29.89	0.929	0.058	20.81	0.883	0.141

artifacts. For the EUVP image, it suggests correcting the blurriness first, and then detects and removes foggy artifacts. To gain a deeper understanding of the image assessment model’s process, we visualize the image embedding distribution of the UDC images and EUVP images in Figure 4. For the UDC images, the original embeddings predominantly span blurry and low-light image areas, indicating the presence of both blur and underexposure. After brightening the images, the embeddings shift towards the blurry image areas. This finding supports our intuitive understanding of the image assessment model and emphasizes our ability to handle the challenging multiple unknown artifacts cases.

4.2. Experiment settings

Datasets Our multi-task pipeline encompasses seven prevalent image quality tasks: denoising, deblurring, super-resolution, low-light enhancement, dehazing, deraining, and deraindrop. For the denoising task, we leverage the SIDD [1] as real image denoising training dataset and synthetic noise dataset with the DIV2K [2] and Flickr2K [32] for synthetic image denoising. For super-resolution, we fol-

low previous practice and train AutoDIR upon DIV2K [2] and Flickr2K [32] training sets, with jointly downsampled images at $\times 8$ and $\times 4$ scales as inputs. For the remaining tasks, we employ specific datasets to train our models. Specifically, we use GoPro [36], LOL [65], RESIDE [28], Rain200L [68], and Raindrop datasets [42] for deblurring, low-light enhancement, dehazing, deraining, and deraindrop tasks respectively. During the inference phase, we evaluate the performance of our pipeline on different test sets. These include the SIDD validation set [1], CBS68 [33], DIV2K validation set [2], GoPro test set [36], HIDE [53], LOL [65], SOTS-Outdoor [28], Rain100 [68], and Raindrop datasets [42], each corresponding to their respective tasks.

Evaluation Metrics The assessment of performance relies upon several metrics. We employ PSNR, SSIM, and the perceptual score LPIP [72] to quantify the results for all the tasks. For the super-resolution and deblurring task, we adopt the widely used blind perceptual metrics including CLIP-IQA [61] and MUSIQ [24] to evaluate the quality of generated images.

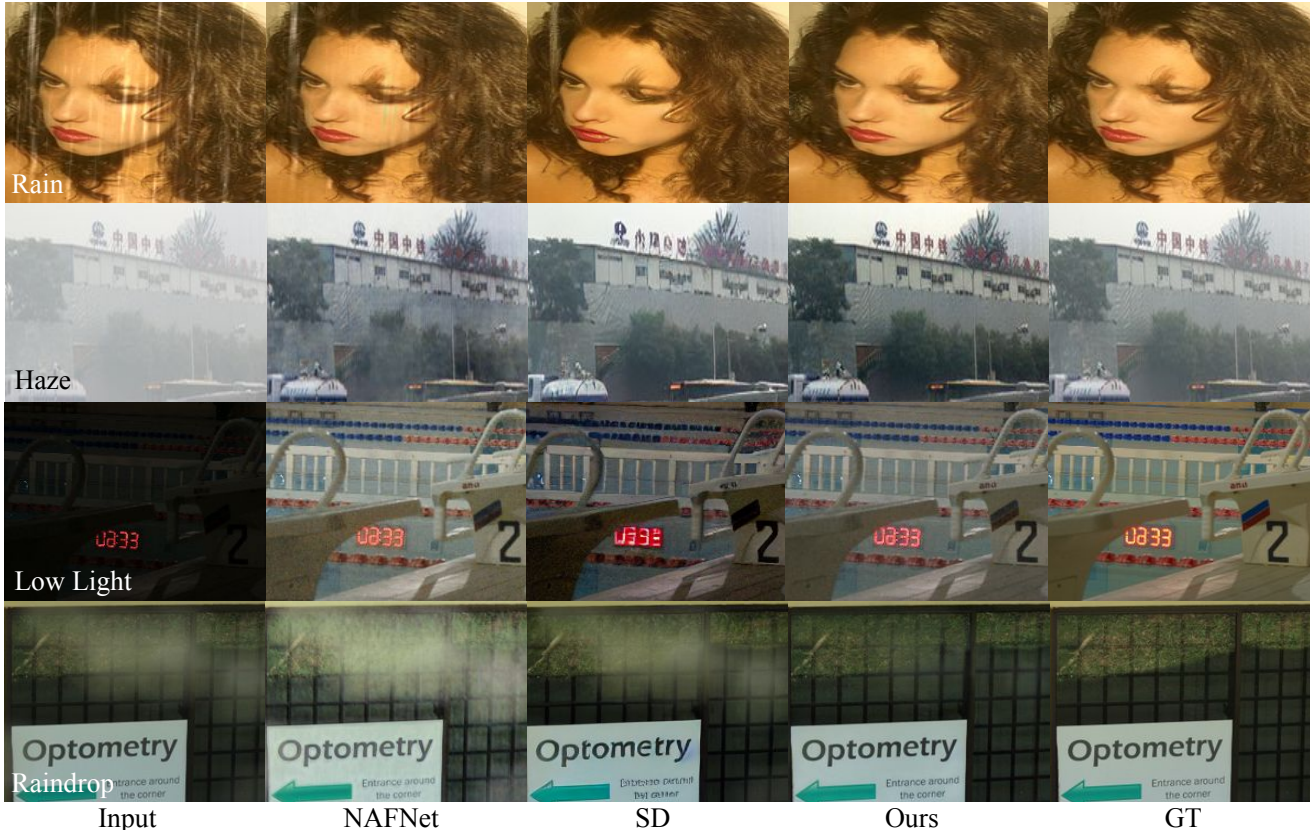


Figure 7. Qualitative comparisons with NAFNet [8] and Stable Diffusion (SD) [48] on deraining, dehaze, low light enhancement and deraindrop tasks. See the Appendix for more results. (Zoom in for better view)

Table 2. Quantitative comparison on deblurring and single image super-resolution x4 and x8 tasks task. PSNR/SSIM/MUSIQ/CLIP-IQA \uparrow : the higher, the better; LPIQ \downarrow : the lower, the better. The best and second-best performances are marked in red and blue.

Method	Deblur										Super Resolution									
	GoPro					HIDE					DIV2k (x4)					DIV2k (x8)				
	PSNR	SSIM	LPIPS	MUSIQ	CLIP-IQA	PSNR	SSIM	LPIPS	MUSIQ	CLIP-IQA	PSNR	SSIM	LPIPS	MUSIQ	CLIP-IQA	PSNR	SSIM	LPIPS	MUSIQ	CLIP-IQA
NAFNet	26.67	0.825	0.208	43.28	0.221	24.66	0.788	0.262	38.02	0.165	28.49	0.784	0.415	39.01	0.347	24.52	0.613	0.554	21.31	0.279
SD	22.53	0.695	0.241	44.83	0.255	22.72	0.709	0.276	40.08	0.2046	27.04	0.767	0.307	39.58	0.366	23.48	0.602	0.380	33.54	0.365
Ours	26.86	0.840	0.156	53.73	0.278	25.26	0.823	0.181	52.68	0.212	27.32	0.778	0.225	52.01	0.501	23.57	0.600	0.301	48.99	0.472

4.3. Results on Multitasking Performance

In this section, we evaluate our approach across seven image restoration and enhancement tasks, with a comparison to both state-of-the-art CNN-based and Diffusion-based methods. Specifically, we conduct comparisons of our results with two state-of-the-art methods: the CNN-based single-task image restoration pipeline NAFNet [8] and the powerful generative backbone Stable Diffusion [48]. Both NAFNet and Stable Diffusion are fine-tuned for all seven tasks, employing an identical training configuration to AutoDIR. Furthermore, we extend our benchmarking efforts to include AirNet [26], a previous state-of-the-art all-in-one method that addresses denoising, deraining, and dehazing tasks simultaneously. By the above comparisons, we aim to evaluate the advancements and improvements achieved by our framework in terms of handling multiple restoration and enhancement tasks.

Summary. Table 1 and Table 2 present quantitative results of AutoDIR and other methods in all seven tasks. As demonstrated, AutoDIR achieves competitive performance across all seven tasks and significantly outperforms both NAFNet [8] and Stable Diffusion [48], as indicated by a substantial margin in the average score. Furthermore, we observe that AutoDIR consistently outperforms AirNet [26], which is trained for three tasks, across most cases. Notably, AutoDIR offers a wider range of supported tasks compared to AirNet [26]. It is important to note that AutoDIR is designed to handle both real and synthetic scenarios. As a result, in certain synthetic benchmarks such as denoising, AutoDIR may achieve comparable or slightly lower scores compared to AirNet [26]. However, it excels in delivering significantly better results for real-world cases. We also show the qualitative comparison results on the seven image restoration tasks in Figure 6 and Figure 7, which demon-

strate that our AutoDIR can achieve more visually appealing results than the other baselines. A comprehensive and detailed analysis of the quantitative and qualitative results for each specific task can be found in the appendix.

4.4. Ablation studies

We performed ablation experiments to validate the importance of the guidance generated by the blind image quality assessment modules (BIQA) and Structural-correction modules (SCM).

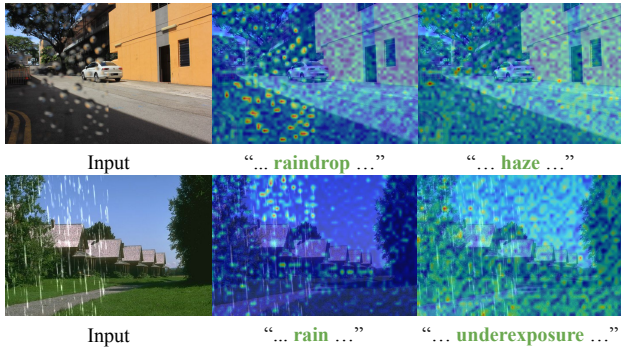


Figure 8. **Cross-attention maps of text-conditioned diffusion image editing.** Left column: input image with raindrop/rain artifact in the left half and no artifact in the right half. Medium column: average attention masks of corresponding keyword “raindrop”/“rain” in the prompt used for editing the input image. Right column: average attention mask for the not-related keyword “haze”/“underexposure” in the prompt used for editing the input image.

How BIQA prompts benefit image restoration? By visualizing the cross-attention in our diffusion model, as shown in Figure 8 (with the right half of the input image as the clean image), we gain insights into the effectiveness of BIQA prompts. Notably, changing the BIQA prompt leads to significant corresponding changes in the cross-attention map. The map closely aligns with the prompt, focusing on specific areas such as raindrops for the “deraindrop” prompt, or evenly distributing attention across the entire image for the “dehazing” prompt. This shows the capability of BIQA prompts to guide the diffusion model’s attention towards regions that are most likely to contain artifacts. As a result, the model can deliver improved restoration results by effectively addressing and correcting the areas of the image that require attention.

Table 3. Ablation study on deraindrop and dehazing tasks. The best results are shown in red.

Method	Deraindrop			Dehaze		
	PSNR	SSIM	LPIPS	PSNR	SSIM	LPIPS
w/o SCM & BIQA	24.84	0.738	0.104	23.49	0.763	0.091
w/o BIQA	28.84	0.923	0.068	27.62	0.959	0.017
w/o SCM	25.58	0.749	0.096	23.60	0.788	0.081
AutoDIR	29.89	0.929	0.058	28.14	0.962	0.021



Figure 9. Qualitative comparisons on w/o and w/ SCM. Without the SCM module, the details e.g. human face, text., are severely distorted, while with the SCM module, the details are well maintained.

Importance of SCM The generative Stable Diffusion model [48] has demonstrated a strong ability to generate unseen features. However, it falls short when it comes to preserving the original structural information of the input image, which is crucial for image enhancement tasks. To address this limitation, we have designed the Structural-correction module. This module aims to preserve the original texture of input images, especially in cases where generative-based models tend to distort fine details such as human faces and text. As illustrated in Figure 9, AutoDIR with the SCM produces high-quality results with fine details intact. On the other hand, the model without the SCM exhibits significant distortion in faces and text. Moreover, these observations are further supported by quantitative comparisons, as shown in Table 3. The model incorporating SCM consistently achieves substantial performance gains across all tasks and metrics. These results provide additional evidence of the crucial role played by the SCM in enhancing the overall performance of the AutoDIR framework.

5. Discussion

We present an all-in-one image restoration with latent diffusion framework (AutoDIR) which can solve complex real-scenario images with multiple unknown degradations. It incorporates a Blind Image Quality Assessment Module (BIQA) and an Automatic Image Refinement Module (AIR) to automatically enhance corrupted images by detecting the dominant degradation. Besides, we introduce a Structural-Correction Module (SCM) to address detail distortion problems caused by latent-diffusion-based models. AutoDIR is the first comprehensive framework for automatic image restoration in the context of complex real-scenario images with multiple unknown degradations. We hope that this framework can provide a solid foundation for further works on complex real-scenario images and has the potential to be extended to various practical applications, such as local image enhancement and multi-task video restoration.

References

- [1] Abdelrahman Abdelhamed, Stephen Lin, and Michael S. Brown. A high-quality denoising dataset for smartphone cameras. In *Proceedings of the IEEE Conference on Computer Vision and Pattern Recognition (CVPR)*, 2018. 7
- [2] Eirikur Agustsson and Radu Timofte. NTIRE 2017 challenge on single image super-resolution: Dataset and study. In *Proceedings of the IEEE Conference on Computer Vision and Pattern Recognition (CVPR) Workshops*, 2017. 7
- [3] David Bau, Hendrik Strobelt, William Peebles, Jonas Wulff, Bolei Zhou, Jun-Yan Zhu, and Antonio Torralba. Semantic photo manipulation with a generative image prior. *ACM Transactions on Graphics (TOG)*, 38(4):59, 2019. 3
- [4] Tim Brooks, Aleksander Holynski, and Alexei A Efros. InstructPix2Pix: Learning to follow image editing instructions. In *Proceedings of Advances in Neural Information Processing Systems (NeurIPS)*, 2023. 3
- [5] Kelvin CK Chan, Xintao Wang, Xiangyu Xu, Jinwei Gu, and Chen Change Loy. GLEAN: Generative latent bank for large-factor image super-resolution. In *Proceedings of the IEEE Conference on Computer Vision and Pattern Recognition (CVPR)*, 2021. 3
- [6] Hila Chefer, Yuval Alaluf, Yael Vinker, Lior Wolf, and Daniel Cohen-Or. Attend-and-excite: Attention-based semantic guidance for text-to-image diffusion models. *ACM Transactions on Graphics (TOG)*, 42(4):1–10, 2023. 3
- [7] Chaofeng Chen, Xinyu Shi, Yipeng Qin, Xiaoming Li, Xiaoguang Han, Tao Yang, and Shihui Guo. Real-world blind super-resolution via feature matching with implicit high-resolution priors. In *IEEE Transactions on Multimedia (TMM)*, 2022. 1
- [8] Liangyu Chen, Xiaojie Chu, Xiangyu Zhang, and Jian Sun. Simple baselines for image restoration. In *Proceedings of European Conferences on Computer Vision (ECCV)*, 2022. 7, 8
- [9] Wei-Ting Chen, Zhi-Kai Huang, Cheng-Che Tsai, Hao-Hsiang Yang, Jian-Jiun Ding, and Sy-Yen Kuo. Learning multiple adverse weather removal via two-stage knowledge learning and multi-contrastive regularization: Toward a unified model. In *Proceedings of the IEEE Conference on Computer Vision and Pattern Recognition (CVPR)*, 2022. 3
- [10] Ben Fei, Zhaoyang Lyu, Liang Pan, Junzhe Zhang, Weidong Yang, Tianyue Luo, Bo Zhang, and Bo Dai. Generative diffusion prior for unified image restoration and enhancement. In *Proceedings of the IEEE Conference on Computer Vision and Pattern Recognition (CVPR)*, 2023. 3
- [11] Sicheng Gao, Xuhui Liu, Bohan Zeng, Sheng Xu, Yanjing Li, Xiaoyan Luo, Jianzhuang Liu, Xiantong Zhen, and Baochang Zhang. Implicit diffusion models for continuous super-resolution. In *Proceedings of the IEEE Conference on Computer Vision and Pattern Recognition (CVPR)*, 2023. 2
- [12] Ian Goodfellow, Jean Pouget-Abadie, Mehdi Mirza, Bing Xu, David Warde-Farley, Sherjil Ozair, Aaron Courville, and Yoshua Bengio. Generative adversarial nets. *Proceedings of Advances in Neural Information Processing Systems (NeurIPS)*, 2014. 2, 3
- [13] Jinjin Gu, Yujun Shen, and Bolei Zhou. Image processing using multi-code GAN prior. In *Proceedings of the IEEE Conference on Computer Vision and Pattern Recognition (CVPR)*, 2020. 3
- [14] Lanqing Guo, Chong Wang, Wenhan Yang, Siyu Huang, Yufei Wang, Hanspeter Pfister, and Bihan Wen. Shadowdiffusion: When degradation prior meets diffusion model for shadow removal. In *Proceedings of the IEEE Conference on Computer Vision and Pattern Recognition (CVPR)*, 2023. 2
- [15] Amir Hertz, Ron Mokady, Jay Tenenbaum, Kfir Aberman, Yael Pritch, and Daniel Cohen-Or. Prompt-to-Prompt image editing with cross attention control. *Proceedings of International Conference on Learning Representations (ICLR)*, 2023. 3
- [16] Jonathan Ho, Ajay Jain, and Pieter Abbeel. Denoising diffusion probabilistic models. *Proceedings of Advances in Neural Information Processing Systems (NeurIPS)*, 2020. 2, 3, 4
- [17] Shady Abu Hussein, Tom Tirer, and Raja Giryes. Image-adaptive GAN based reconstruction. In *Proceedings of the AAAI Conference on Artificial Intelligence*, 2020. 3
- [18] Md Jahidul Islam, Youya Xia, and Junaed Sattar. Fast underwater image enhancement for improved visual perception. *IEEE Robotics and Automation Letters ((RA-L))*, 2020. 6
- [19] Seo-Won Ji, Jeongmin Lee, Seung-Wook Kim, Jun-Pyo Hong, Seung-Jin Baek, Seung-Won Jung, and Sung-Jea Ko. XYDeblur: divide and conquer for single image deblurring. In *Proceedings of the IEEE Conference on Computer Vision and Pattern Recognition (CVPR)*, 2022. 1
- [20] Chao Jia, Yinfei Yang, Ye Xia, Yi-Ting Chen, Zarana Parekh, Hieu Pham, Quoc Le, Yun-Hsuan Sung, Zhen Li, and Tom Duerig. Scaling up visual and vision-language representation learning with noisy text supervision. In *Proceedings of International Conference on Machine Learning (ICML)*, 2021. 2
- [21] Kui Jiang, Zhongyuan Wang, Peng Yi, Chen Chen, Baojin Huang, Yimin Luo, Jiayi Ma, and Junjun Jiang. Multi-scale progressive fusion network for single image deraining. In *Proceedings of the IEEE Conference on Computer Vision and Pattern Recognition (CVPR)*, 2020. 1
- [22] Bahjat Kawar, Michael Elad, Stefano Ermon, and Jiaming Song. Denoising diffusion restoration models. In *Proceedings of Advances in Neural Information Processing Systems (NeurIPS)*, 2022. 2, 3
- [23] Bahjat Kawar, Shiran Zada, Oran Lang, Omer Tov, Huiwen Chang, Tali Dekel, Inbar Mosseri, and Michal Irani. Magic: Text-based real image editing with diffusion models. In *Proceedings of the IEEE Conference on Computer Vision and Pattern Recognition (CVPR)*, 2023. 3
- [24] Junjie Ke, Qifei Wang, Yilin Wang, Peyman Milanfar, and Feng Yang. MUSIQ: Multi-scale image quality transformer. In *Proceedings of the IEEE International Conference on Computer Vision (ICCV)*. 7
- [25] Diederik P Kingma and Max Welling. Auto-encoding variational bayes. 2014. 2, 4
- [26] Boyun Li, Xiao Liu, Peng Hu, Zhongqin Wu, Jiancheng Lv, and Xi Peng. All-In-One image restoration for unknown cor-

- ruption. In *Proceedings of the IEEE Conference on Computer Vision and Pattern Recognition (CVPR)*, 2022. 2, 3, 8
- [27] Boyun Li, Xiao Liu, Peng Hu, Zhongqin Wu, Jiancheng Lv, and Xi Peng. All-in-One image restoration for unknown corruption. In *Proceedings of the IEEE Conference on Computer Vision and Pattern Recognition (CVPR)*, 2022. 3
- [28] Boyi Li, Wenqi Ren, Dengpan Fu, Dacheng Tao, Dan Feng, Wenjun Zeng, and Zhangyang Wang. Benchmarking single-image dehazing and beyond. *IEEE Transactions on Image Processing (TIP)*, 2018. 5, 6, 7
- [29] Dasong Li, Xiaoyu Shi, Yi Zhang, Ka Chun Cheung, Simon See, Xiaogang Wang, Hongwei Qin, and Hongsheng Li. A simple baseline for video restoration with grouped spatial-temporal shift. In *Proceedings of the IEEE Conference on Computer Vision and Pattern Recognition (CVPR)*, 2023. 1
- [30] Junnan Li, Dongxu Li, Caiming Xiong, and Steven Hoi. BLIP: Bootstrapping language-image pre-training for unified vision-language understanding and generation. In *Proceedings of International Conference on Machine Learning (ICML)*, 2022. 2
- [31] Ruoteng Li, Robby T Tan, and Loong-Fah Cheong. All-in-One bad weather removal using architectural search. In *Proceedings of the IEEE Conference on Computer Vision and Pattern Recognition (CVPR)*, 2020. 3
- [32] Bee Lim, Sanghyun Son, Heewon Kim, Seungjun Nah, and Kyoung Mu Lee. Enhanced deep residual networks for single image super-resolution. In *Proceedings of the IEEE Conference on Computer Vision and Pattern Recognition (CVPR) Workshops*, 2017. 7
- [33] D. Martin, C. Fowlkes, D. Tal, and J. Malik. A database of human segmented natural images and its application to evaluating segmentation algorithms and measuring ecological statistics. In *Proceedings of the IEEE International Conference on Computer Vision (ICCV)*, 2001. 7
- [34] Sachit Menon, Alexandru Damian, Shijia Hu, Nikhil Ravi, and Cynthia Rudin. PULSE: Self-supervised photo upsampling via latent space exploration of generative models. In *Proceedings of the IEEE Conference on Computer Vision and Pattern Recognition (CVPR)*, 2020. 3
- [35] Yao Mingde, Huang Jie, Jin Xin, Xu Ruikang, Zhou Shenglong, Zhou Man, , and Xiong Zhiwei. Generalized lightness adaptation with channel selective normalization. In *Proceedings of the IEEE International Conference on Computer Vision (ICCV)*, 2023. 1
- [36] Seungjun Nah, Tae Hyun Kim, and Kyoung Mu Lee. Deep multi-scale convolutional neural network for dynamic scene deblurring. In *Proceedings of the IEEE Conference on Computer Vision and Pattern Recognition (CVPR)*, 2017. 7
- [37] Alex Nichol, Prafulla Dhariwal, Aditya Ramesh, Pranav Shyam, Pamela Mishkin, Bob McGrew, Ilya Sutskever, and Mark Chen. GLIDE: Towards photorealistic image generation and editing with text-guided diffusion models. 2021. 3
- [38] Ozan Özdenizci and Robert Legenstein. Restoring vision in adverse weather conditions with patch-based denoising diffusion models. *IEEE Transactions on Pattern Analysis and Machine Intelligence (TPAMI)*, 2023. 2
- [39] Xingang Pan, Xiaohang Zhan, Bo Dai, Dahua Lin, Chen Change Loy, and Ping Luo. Exploiting deep generative prior for versatile image restoration and manipulation. *IEEE Transactions on Pattern Analysis and Machine Intelligence (TPAMI)*, 44(11):7474–7489, 2021. 2, 3
- [40] Dongwon Park, Byung Hyun Lee, and Se Young Chun. All-in-One image restoration for unknown degradations using adaptive discriminative filters for specific degradations. In *Proceedings of the IEEE Conference on Computer Vision and Pattern Recognition (CVPR)*, 2023. 2, 3
- [41] Rui Qian, Robby T Tan, Wenhan Yang, Jiajun Su, and Jiaying Liu. Attentive generative adversarial network for rain-drop removal from a single image. In *Proceedings of the IEEE Conference on Computer Vision and Pattern Recognition (CVPR)*, 2018. 1
- [42] Rui Qian, Robby T Tan, Wenhan Yang, Jiajun Su, and Jiaying Liu. Attentive generative adversarial network for rain-drop removal from a single image. In *Proceedings of the IEEE Conference on Computer Vision and Pattern Recognition (CVPR)*, 2018. 7
- [43] Xu Qin, Zhilin Wang, Yuanchao Bai, Xiaodong Xie, and Huizhu Jia. FFA-Net: Feature fusion attention network for single image dehazing. In *Proceedings of the AAAI Conference on Artificial Intelligence*, 2020. 1
- [44] Yuhui Quan, Mingqin Chen, Tongyao Pang, and Hui Ji. Self2Self with dropout: Learning self-supervised denoising from single image. In *Proceedings of the IEEE Conference on Computer Vision and Pattern Recognition (CVPR)*, 2020. 1
- [45] Alec Radford, Jong Wook Kim, Chris Hallacy, Aditya Ramesh, Gabriel Goh, Sandhini Agarwal, Girish Sastry, Amanda Askell, Pamela Mishkin, Jack Clark, et al. Learning transferable visual models from natural language supervision. In *Proceedings of International Conference on Machine Learning (ICML)*, 2021. 2, 3, 4
- [46] Aditya Ramesh, Prafulla Dhariwal, Alex Nichol, Casey Chu, and Mark Chen. Hierarchical text-conditional image generation with clip latents. *arXiv preprint arXiv:2204.06125*, 2022. 3
- [47] Dongwei Ren, Wangmeng Zuo, Qinghua Hu, Pengfei Zhu, and Deyu Meng. Progressive image deraining networks: A better and simpler baseline. In *Proceedings of the IEEE Conference on Computer Vision and Pattern Recognition (CVPR)*, 2019. 1
- [48] Robin Rombach, Andreas Blattmann, Dominik Lorenz, Patrick Esser, and Björn Ommer. High-resolution image synthesis with latent diffusion models. In *Proceedings of the IEEE Conference on Computer Vision and Pattern Recognition (CVPR)*, 2022. 2, 3, 4, 5, 7, 8, 9
- [49] Olaf Ronneberger, Philipp Fischer, and Thomas Brox. U-Net: Convolutional networks for biomedical image segmentation. In *Proceedings of Medical Image Computing and Computer-Assisted Intervention (MICCAI)*, 2015. 5
- [50] Chitwan Saharia, William Chan, Huiwen Chang, Chris Lee, Jonathan Ho, Tim Salimans, David Fleet, and Mohammad Norouzi. Palette: Image-to-image diffusion models. In *ACM SIGGRAPH Conference Proceedings*, 2022. 2

- [51] Chitwan Saharia, William Chan, Saurabh Saxena, Lala Li, Jay Whang, Emily L Denton, Kamyar Ghasemipour, Raphael Gontijo Lopes, Burcu Karagol Ayan, Tim Salimans, et al. Photorealistic text-to-image diffusion models with deep language understanding. *Proceedings of Advances in Neural Information Processing Systems (NeurIPS)*, 2022. 3
- [52] Chitwan Saharia, Jonathan Ho, William Chan, Tim Salimans, David J Fleet, and Mohammad Norouzi. Image super-resolution via iterative refinement. *IEEE Transactions on Pattern Analysis and Machine Intelligence (TPAMI)*, 2022. 2
- [53] Ziyi Shen, Wenguan Wang, Jianbing Shen, Haibin Ling, Tingfa Xu, and Ling Shao. Human-aware motion deblurring. In *Proceedings of the IEEE International Conference on Computer Vision (ICCV)*, 2019. 7
- [54] Yuda Song, Zhuqing He, Hui Qian, and Xin Du. Vision transformers for single image dehazing. *IEEE Transactions on Image Processing (TIP)*, 2023. 1
- [55] Hao Tan and Mohit Bansal. LXMERT: Learning cross-modality encoder representations from transformers. *Proceedings of the 2019 Conference on Empirical Methods in Natural Language Processing (EMNLP)*, 2019. 2
- [56] Ming Tao, Hao Tang, Fei Wu, Xiao-Yuan Jing, Bing-Kun Bao, and Changsheng Xu. DF-GAN: A simple and effective baseline for text-to-image synthesis. In *Proceedings of the IEEE Conference on Computer Vision and Pattern Recognition (CVPR)*, 2022. 2, 3
- [57] Ming-Feng Tsai, Tie-Yan Liu, Tao Qin, Hsin-Hsi Chen, and Wei-Ying Ma. FRank: a ranking method with fidelity loss. In *ACM SIGGRAPH Conference Proceedings*, 2007. 4
- [58] Arash Vahdat and Jan Kautz. Nvae: A deep hierarchical variational autoencoder. *Proceedings of Advances in Neural Information Processing Systems (NeurIPS)*, 2020. 2
- [59] Jeya Maria Jose Valanarasu, Rajeev Yasarla, and Vishal M Patel. Transweather: Transformer-based restoration of images degraded by adverse weather conditions. In *Proceedings of the IEEE Conference on Computer Vision and Pattern Recognition (CVPR)*, 2022. 3
- [60] Ashish Vaswani, Noam Shazeer, Niki Parmar, Jakob Uszkoreit, Llion Jones, Aidan N Gomez, Łukasz Kaiser, and Illia Polosukhin. Attention is all you need. *Proceedings of Advances in Neural Information Processing Systems (NeurIPS)*, 2017. 5
- [61] Jianyi Wang, Kelvin CK Chan, and Chen Change Loy. Exploring CLIP for assessing the look and feel of images. In *Proceedings of the AAAI Conference on Artificial Intelligence*, 2023. 7
- [62] Jianyi Wang, Zongsheng Yue, Shangchen Zhou, Kelvin CK Chan, and Chen Change Loy. Exploiting diffusion prior for real-world image super-resolution. In *arXiv preprint arXiv:2305.07015*, 2023. 1, 2
- [63] Jianyi Wang, Zongsheng Yue, Shangchen Zhou, Kelvin CK Chan, and Chen Change Loy. Exploiting diffusion prior for real-world image super-resolution. *arXiv preprint arXiv:2305.07015*, 2023. 2
- [64] Yinhuai Wang, Jiwen Yu, and Jian Zhang. Zero-shot image restoration using denoising diffusion null-space model. In *Proceedings of International Conference on Learning Representations (ICLR)*, 2023. 2, 3
- [65] Chen Wei, Wenjing Wang, Wenhan Yang, and Jiaying Liu. Deep retinex decomposition for low-light enhancement. *Proceedings of The British Machine Vision Conference (BMVC)*, 2018. 7
- [66] Tao Xu, Pengchuan Zhang, Qiuyuan Huang, Han Zhang, Zhe Gan, Xiaolei Huang, and Xiaodong He. AttnGAN: Fine-grained text to image generation with attentional generative adversarial networks. In *Proceedings of the IEEE Conference on Computer Vision and Pattern Recognition (CVPR)*, 2018. 2, 3
- [67] Tao Yang, Peiran Ren, Xuansong Xie, and Lei Zhang. GAN prior embedded network for blind face restoration in the wild. In *Proceedings of the IEEE Conference on Computer Vision and Pattern Recognition (CVPR)*, 2021. 3
- [68] Wenhan Yang, Robby T Tan, Jiashi Feng, Jiaying Liu, Zongming Guo, and Shuicheng Yan. Deep joint rain detection and removal from a single image. In *Proceedings of the IEEE Conference on Computer Vision and Pattern Recognition (CVPR)*, 2017. 7
- [69] Hui Ye, Xiulong Yang, Martin Takac, Rajshekhar Sunderraman, and Shihao Ji. Improving text-to-image synthesis using contrastive learning. *Proceedings of The British Machine Vision Conference (BMVC)*, 2021. 2, 3
- [70] Han Zhang, Jing Yu Koh, Jason Baldridge, Honglak Lee, and Yinfei Yang. Cross-modal contrastive learning for text-to-image generation. In *Proceedings of the IEEE Conference on Computer Vision and Pattern Recognition (CVPR)*, 2021. 2, 3
- [71] Jinghao Zhang, Jie Huang, Mingde Yao, Zizheng Yang, Hu Yu, Man Zhou, and Feng Zhao. Ingredient-oriented multi-degradation learning for image restoration. In *Proceedings of the IEEE Conference on Computer Vision and Pattern Recognition (CVPR)*, 2023. 2, 3
- [72] Richard Zhang, Phillip Isola, Alexei A Efros, Eli Shechtman, and Oliver Wang. The unreasonable effectiveness of deep features as a perceptual metric. In *Proceedings of the IEEE Conference on Computer Vision and Pattern Recognition (CVPR)*, 2018. 7
- [73] Zhixing Zhang, Ligong Han, Arnab Ghosh, Dimitris N Metaxas, and Jian Ren. SINE: Single image editing with text-to-image diffusion models. In *Proceedings of the IEEE Conference on Computer Vision and Pattern Recognition (CVPR)*, 2023. 3
- [74] Zhaoyang Zhang, Yitong Jiang, Jun Jiang, Xiaogang Wang, Ping Luo, and Jinwei Gu. STAR: A structure-aware lightweight transformer for real-time image enhancement. In *Proceedings of the IEEE International Conference on Computer Vision (ICCV)*, 2021. 1
- [75] Zhaoyang Zhang, Yitong Jiang, Wenqi Shao, Xiaogang Wang, Ping Luo, Kaimo Lin, and Jinwei Gu. Real-time controllable denoising for image and video. In *Proceedings of the IEEE Conference on Computer Vision and Pattern Recognition (CVPR)*, 2023. 1
- [76] Yuqian Zhou, David Ren, Neil Emerton, Sehoon Lim, and Timothy Large. Image restoration for under-display camera.

In *Proceedings of the IEEE Conference on Computer Vision and Pattern Recognition (CVPR)*, 2021. 6

- [77] Yuqian Zhou, David Ren, Neil Emerton, Sehoon Lim, and Timothy Large. Image restoration for under-display camera. *Proceedings of the IEEE Conference on Computer Vision and Pattern Recognition (CVPR)*, 2021. 6
- [78] Minfeng Zhu, Pingbo Pan, Wei Chen, and Yi Yang. DM-GAN: Dynamic memory generative adversarial networks for text-to-image synthesis. In *Proceedings of the IEEE Conference on Computer Vision and Pattern Recognition (CVPR)*, 2019. 3
- [79] Yuanzhi Zhu, Kai Zhang, Jingyun Liang, Jiezhong Cao, Bihan Wen, Radu Timofte, and Luc Van Gool. Denoising diffusion models for plug-and-play image restoration. In *Proceedings of the IEEE Conference on Computer Vision and Pattern Recognition (CVPR)*, 2023. 2